Enhanced Generation of Reactive Radicals and Electrocatalytic Oxidation of Levofloxacin Using a Trimetallic CuFeV Layered Double Hydroxide-Containing Electrode

Ramazan Keyikoğlu [a,b], Alireza Khataee [a,c,*], Yeojoon Yoon [d,*]

[a] Department of Environmental Engineering, Gebze Technical University, 41400 Gebze, Turkey

[b] Department of Environmental Engineering, Helmholtz Centre for Environmental Research – UFZ, 04318 Leipzig, Germany

[c] Research Laboratory of Advanced Water and Wastewater Treatment Processes, Department of Applied Chemistry, Faculty of Chemistry, University of Tabriz, 51666−16471 Tabriz, Iran

[d] Department of Environmental and Energy Engineering, Yonsei University, Wonju, Republic of Korea

* Corresponding author: akhataee@gtu.edu.tr; yajoony@yonsei.ac.kr

Abstract

In Electro-Fenton (EF) processes, the use of iron as a catalyst under acidic conditions results in increased costs and potential secondary pollution. To address these issues, we developed a CuFeV layered double hydroxide (LDH) coating on graphite felt (GF) (CuFeV LDH@GF) that offers an effective performance across a broad pH range without causing metal pollution. The CuFeV LDH@GF cathode exhibited a good oxygen reduction performance, high stability, and an efficient removal of levofloxacin (LEV) over a wide pH range (pH = 3–10). The simultaneous presence of Cu^{2+}/Cu^{3+}, Fe^{2+}/Fe^{3+}, and V^{4+}/V^{5+} redox pairs played a crucial role in facilitating interfacial electron transfer, thereby enhancing the production and subsequent activation of H_2O_2 within the system. The rate constant (k_{app}) of LEV removal under neutral conditions with the CuFeV LDH@GF electrode was more than two times that of the raw GF electrode. This improvement can be attributed to the CuFeV LDH coating, which increased the generation of hydroxyl radicals ($^{\bullet}OH$) from 0.64 to 1.27 mM. Importantly, the CuFeV LDH@GF electrode maintained its efficiency and stability even after 10 reuse cycles. Additionally, GC–MS analyses revealed the degradation of intermediate compounds, which include cyclic and aliphatic compounds. This study provides significant insights into the synergistic effects of trimetallic LDHs, contributing to the development of high-performance cathodes.

Keywords: Electrophoretic deposition; Emerging contaminant; Electro-Fenton; Graphite felt; Water treatment.

1. Introduction

Concerns regarding the global effects of pharmaceuticals on water resources are increasing because the active components of these chemicals may remain unaffected or become highly toxic after treatment by conventional wastewater treatment facilities [1]. Levofloxacin (LEV) belongs to the class of fluoroquinolones and is frequently detected in hospital and pharmaceutical wastewater. The existence of a strong C-F covalent bond in its structure results in toxic and refractory degradation intermediates during the decomposition [2]. Furthermore, the potent antibacterial properties and limited metabolism of LEV contribute to the accumulation of pollutants, even after wastewater treatment. Advanced oxidation processes (AOPs), which are fast and effective methods for treating water contaminated with persistent organic pollutants, such as pharmaceuticals, have been proposed [3]. The Fenton/Fenton-like processes, which are a class of AOPs, generate hydroxyl radicals (•OH) through the reaction between M^{+2} (transition metals, such as Fe, Co, and Cu), and hydrogen peroxide at very low pH levels (2.8–3.5) [4]. The electro-Fenton (EF) process has received significant attention as it can electrochemically produce H_2O_2, eliminating the need for the storage and handling of hazardous H_2O_2 [5]. As in the classical Fenton process, M^{2+} acts as a catalyst, producing •OH radicals that can break down pollutants. EF process also regenerates M^{3+} via cathodic reduction, further improving the overall efficiency [6]. By employing heterogeneous catalysts, the challenges associated with homogeneous catalysts in EF processes, such as waste sludge formation and a limited working pH range, can be overcome [7,8].

Layered double hydroxides (LDHs) are a type of inorganic nanomaterial that belongs to the anionic clay family. They have a two-dimensional layered structure, which is represented by the general formula of $[M^{2+}_{1-x}M^{3+}_{x}OH_2]^{x+}[A^{n-}_{x/n}.yH_2O]^{x-}$, where M^{2+} and M^{3+} denote divalent and trivalent cations, respectively; x indicates the molar ratio of $M^{3+}/(M^{3+} + M^{2+})$; A^{n-} is an

anion; and y is the number of water molecules located between the layers [9]. LDHs consist of positively charged cationic layers, similar to brucite, along with interlayer hydrated anions that compensate for the overall charge. These materials have demonstrated significant catalytic activities owing to their large surface areas, abundant catalytic active sites, and stability [10]. Furthermore, researchers have recently investigated the diverse catalytic capabilities of LDHs in heterogeneous Fenton processes [11,12].

A FeIIFeIII LDH was grown on a carbon-felt electrode for the EF process, which exhibited a synergistic effect resulting from both homogeneous and heterogeneous H_2O_2 activation [13]. However, the catalytic sites of iron species in a singular metal oxide phase are not efficiently utilized to produce $^{\bullet}OH$ in the heterogenous EF process, indicating the possibilities for further improvements. Incorporating a transition metal into a Fe-based LDH can increase its catalytic activity by promoting electron transfer rates. Additionally, third-metal doping expands the operating pH range and minimizes heavy metal leaching [14]. The presence of Co^{2+}/Co^{3+}, Fe^{2+}/Fe^{3+}, and Ce^{3+}/Ce^{4+} redox couples in the EF process involving a CoFeCe LDH significantly enhances interfacial electron exchange, thereby facilitating the production and activation of H_2O_2 to generate reactive radicals [15]. Similarly, vanadium is a transition metal that possesses several valence states (V^{3+}, V^{4+}, and V^{5+}). Recent research has demonstrated that different vanadium oxides (such as V_2O_3, VO_2, and V_2O_5) can stimulate H_2O_2 to achieve an effective degradation of contaminants [16,17].

Energy consumption is a major limitation of EF process, as the generation of reactive oxygen species requires elevated potentials. Additionally, optimal performance is typically restricted to acidic conditions due to the pH dependence of the Fenton reaction. In this study, to overcome these challenges, we aimed to develop CuFeV layered double hydroxide incorporated graphite felt (CuFeV@GF) electrode through electrophoretic deposition (EPD) method. The integration of LDH particles into the GF matrix offers multiple active sites for H_2O_2 adsorption and

subsequent decomposition, minimizing limitations caused by mass transfer in •OH formation. Moreover, the use of CuFeV@GF cathode was expected to minimize electricity consumption, contributing to improved energy efficiency and sustainability for large-scale applications. We evaluated the performance of the EF process using the CuFeV LDH@GF electrode in removing LEV and examined the influence of process parameters, such as the LEV concentration, pH, and applied voltage, on the electrode performance. Furthermore, we investigated the degradation mechanism of LEV during the CuFeV LDH@GF–EF process. The stable performance of the CuFeV LDH under near-neutral conditions with prolonged catalytic activity makes it a promising solution for efficient and eco-friendly wastewater treatment.

2. Materials and methods

2.1. Materials

Vanadium (III) chloride (97%), Copper(II) chloride dihydrate (≥99.0%), hydrogen peroxide (30%), Iron (III) chloride hexahydrate (≥99%), nitric acid (70%), sodium hydroxide (99%), $Mg(NO_3)_2.6H_2O$ (%99), diethyl ether, N, O–bis–(trimethylsilyl)–acetamide (≥95%), o–phenylenediamine (OPD, 99.5%), and ammonium molybdate tetrahydrate (≥99.0%) were obtained from Merck, Germany. GF (Sigratherm) was provided by SGL CARBON (Germany). Platinum plate was provided by DiaCCon GmbH (Germany).

2.2. Fabrication of the CuFeV LDH@GF electrode

The CuFeV LDH was obtained via a co-precipitation reaction as described in our previous paper [18]. Specifically, certain amounts of $CuCl_2.2H_2O$, $FeCl_3 \cdot 6H_2O$, and VCl_3 (M^{2+}/M^{3+} = 3) were added to 40 mL ultrapure water, which had been previously purged with N_2. The pH of the solution was gradually raised to 8 by adding NaOH, while maintaining constant stirring. Following a 24 h aging period, centrifugation was performed to obtain the solid phase. Finally,

109 the resulting sample was treated multiple times with deionized (DI) water to remove impurities
110 before it was placed in an oven (BINDER GmbH, Germany) at 50 °C for 7 h.
111 In this study, EPD was employed to deposit LDH nanoparticles onto GF, as shown in Figure
112 1a [19]. Prior to the process, the GF was subjected to a cleaning process involving
113 ultrasonication (Elmasonic P120H, 37 kHz, Germany) in ethanol, acetone, and DI water, with
114 each step lasting 15 min. Afterward, the pretreated GF was subjected to a hydrothermal acid
115 treatment using concentrated HNO_3 at 90 °C for 9 h. To prepare a colloidal suspension of LDH,
116 0.5 g of LDH and $Mg(NO_3)_2 \cdot 6H_2O$ were added to 20 mL of 2-propanol. Thereafter, the
117 suspension was subjected to ultrasonic treatment in a bath for 0.5 h to ensure uniform dispersion
118 of LDH particles. Thereafter, the mixture was placed into an electrochemical cell connected to
119 a direct current (DC) power source. The positive and negative terminals were connected to the
120 GF and stainless steel (SS, 316 AISI SS, Turkey) electrodes, which had been vertically inserted
121 into the cell. Finally, LDH particles were electrodeposited onto the GF surface using a voltage
122 of 40 V for 7 min. The resulting electrode with CuFeV LDH coating was designated as CuFeV
123 LDH@GF.

124 **2.3. Characterization studies**

125 The characterization methods of the catalyst are detailed in Text S1. To study the
126 electrochemical behavior of the CuFeV LDH@GF electrode, a three-electrode potentiostat
127 (Metrohm Autolab PGSTAT302N, the Netherlands) with a saturated calomel electrode (SCE),
128 a platinum wire, and the coated electrode served as reference, counter, and working electrodes,
129 respectively. The cyclic voltammetry (CV) and linear sweep voltammetry (LSV) tests were
130 conducted at a scan rate of 30 mV s^{-1} in 0.05 M Na_2SO_4 solution at pH = 6.8.

131 The procedures for determining cathodic H_2O_2 production and $^{\bullet}OH$ during the process are
132 provided in Text S2. Gas chromatography/mass spectrometry (GC–MS) was performed using

an Agilent 6890N instrument (USA) to detect the degradation intermediates of LEV (Text S3). The heavy metal leaching from the CuFeV LDH during the reaction was evaluated through inductively coupled plasma–optical emission spectrometry (ICP–OES) using a Perkin-Elmer Optima 7000 DV instrument (USA).

2.4. Activity of the CuFeV LDH@GF electrode during the EF process

EF tests were performed in a 150 mL glass cell. CuFeV LDH@GF (6 cm x 5 cm) and Pt (6 cm x 5 cm) plates were vertically placed parallel to each other with a gap of 1.5 cm. The reactor was powered by a DC power supply (Aim-TTi TSX3510, UK). Experiments were conducted in a 100 mL of LEV solution containing 50 mM Na_2SO_4 as the supporting electrolyte. Additionally, O_2 gas was bubbled from the bottom of the CuFeV LDH@GF electrode for in-situ H_2O_2 generation. The LEV concentrations in the solutions were determined via ultraviolet–visible (UV–vis) spectroscopy (Hach Lange DR 3900) at a wavelength of 288 nm. The synergy factor (SF) of the process was computed using Eq. 1.

$$SF = \frac{\mathrm{k_{app}(CuFeV\ LDH@GF - EF)}}{\mathrm{k_{app}(Raw\ GF - EF) + k_{app}\ (Adsorption)}} \quad (1)$$

where k_{app} is the pseudo-first-order rate constant. Energy consumption (EC) during LEV degradation in the CuFeV LDH@GF–EF process was calculated using Eqs. 2 and 3 [6].

$$\mathrm{EC\ (kWh\ m^{-3})} = \frac{\mathrm{U \times i \times t}}{10^3 \times \mathrm{V}} \quad (2)$$

$$\mathrm{EC\ (kWh\ kg^{-1})} = \frac{\mathrm{U \times i \times t}}{10^3 \times \mathrm{V} \times (C_0 - C_t)} \quad (3)$$

where i is the current (A); U is the voltage (V); t is the reaction duration (h); V (m^3) is the volume of LEV solution; and C_0 and C_t (kg/m^3) are the LEV concentrations in the beginning of the process and at a given moment, respectively.

3. Results and discussion

3.1. Characterization tests

The X-ray diffraction (XRD) pattern of the CuFeV LDH reveals a highly crystalline material, as illustrated by the prominent peaks in Figure 1b. The characteristic peaks, including those of (003), (006), and (009) planes, originate from the lamellar structure and stacking planes of LDH structures [20,21]. Based on the Debye–Scherrer calculations, the CuFeV LDH had an average crystallite size of 23.4 nm. Using the Bragg equation, the basal spacing (d_{003}) of the CuFeV LDH is calculated as 6.87 Å, which is consistent with the results obtained for LDHs prepared with the same molar ratio of M(II)/M(III) [20]. The diffraction peaks and the basal reflections of CuFeV were indexed to the hexagonal unit cell of a 3 R rhombohedral system with a space group of R3m [22].

Fourier transform infrared (FTIR) spectrum of the CuFeV LDH shows a broad absorption band at 3000–3650 cm^{-1}, originating from the OH stretching vibration related to interlayer water and the metal hydroxide layers [21] (Figure 1c). Moreover, the band centered at 1622 cm^{-1} corresponds to the angular deformation of water molecules [23]. A series of bands between 400 and 1000 cm^{-1} are observed owing to the lattice vibrations of M–O and O–M–O (M: Cu, Fe or V) stretching modes [24]. These polymetallic M–O and O–M–O linkages are crucial in the electron transfer among Cu, Fe, and V during the activation of H_2O_2 in the EF process.

Transmission electron microscopy (TEM)–energy dispersive X-ray spectroscopy (EDS) elemental mapping analyses of the catalyst demonstrate the uniform distribution of Cu, Fe, V, Cl, C, and O elements, as shown in Figure 1d. Impurities were not detected in the mapping analysis. The TEM images further reveal a plate-like morphology, which is a characteristic of layered double hydroxides, as depicted in Figure 1e. The analysis of the (009) lattice plane reveals an interplanar spacing of 0.26 nm, as illustrated in Figure 1f.

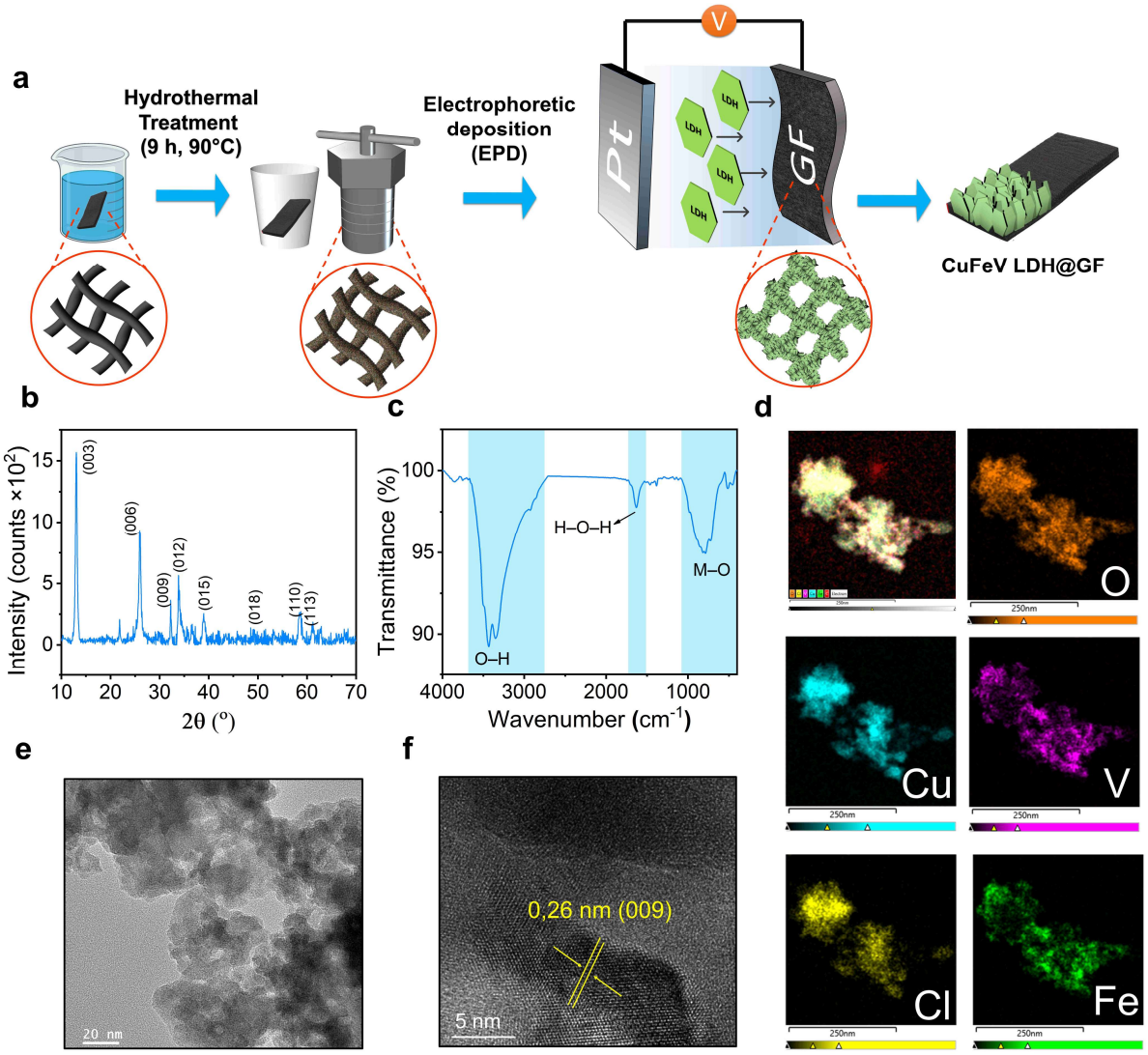

Figure 1. a) Illustration of the production of CuFeV LDH@GF via EPD; b) powder XRD pattern, c) FTIR spectrum, d) EDS elemental mapping, and e) high-resolution TEM image of the CuFeV LDH (inset shows the lattice spacing).

The Brunauer–Emmett–Teller (BET) surface area (S_{BET}), total pore volume, and average pore diameter of the CuFeV LDH were 113.92 m^2/g, 0.53 cm^3/g, and 18.63 nm, respectively. Complete coverage of GF filaments by the CuFeV LDH was apparent in the SEM images (Figure 2). The thin sheet-like LDH particles uniformly grew on the GF vertically without aggregation. These characteristics provide abundant active sites for catalytic reactions, allowing for efficient LEV adsorption and degradation.

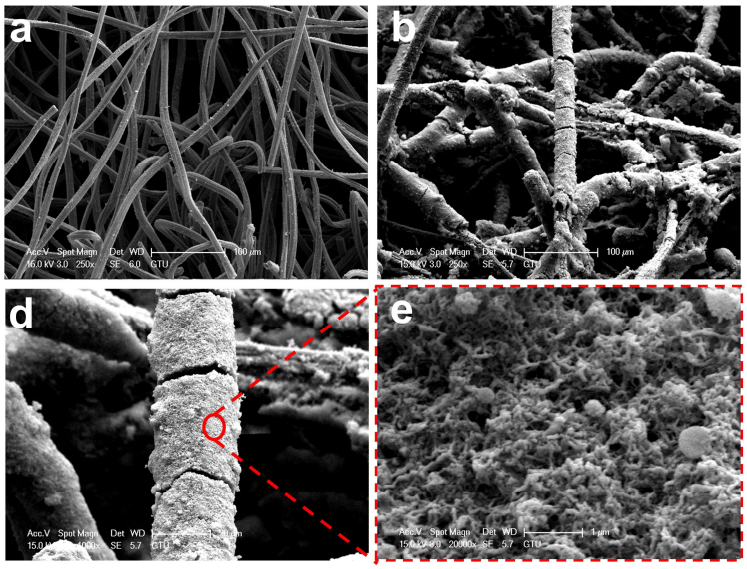

Figure 2. Scanning electron microscopy (SEM) images of a) raw GF and b–e) CuFeV LDH@GF at different magnifications.

X-ray photoelectron spectroscopy (XPS) was utilized to investigate the surface chemistry of the CuFeV LDH. The Fe 2p XPS spectrum showed two peaks at binding energies of 711.9 and 724.8 eV, which are separated by a binding energy of 13 eV, corresponding to the $2p_{3/2}$ and $2p_{1/2}$ spin state of Fe^{3+} (Figure 3a) [25]. A narrow Cu 2p scan showed spin-orbit peaks of Cu $2p_{3/2}$ and Cu $2p_{1/2}$ as well as two satellite peaks (Figure 3b). Cu $2p_{3/2}$ (at 933.1 and 935.1 eV) and Cu $2p_{1/2}$ (at 953.1 and 955.1 eV) peaks indicated the existence of Cu^{2+} species in the LDH [24]. The V 2p spectrum contained two peaks corresponding to V $2p_{3/2}$ and V $2p_{1/2}$, which are separated by 7.2 eV spin-orbit splitting. Three V $2p_{3/2}$ peaks at 515.3, 515.8, and 517.2 eV were attributed to V^{3+}, V^{4+}, and V^{5+} species, respectively (Figure 3c) [26]. The partial oxidation of V^{3+} during the synthesis and the presence of multivalent V species have been reported for V-doped LDHs [27]. The three components that comprised the O 1s peak were detected at 530.4, 531.7, and 532.4 eV, representing lattice oxygen, chemisorbed and dissociated oxygen, and surface OH– groups of metal centers, respectively (Figure 3d) [27]. The coexistence of various oxidation states for metal constituents of the CuFeV supports multiple redox reactions, enhancing the generation of ROS and promoting efficient pollutant degradation.

The electrochemical behaviors of CuFeV LDH@GF and raw GF electrodes were analyzed using CV, as shown in Figure 3e. Comparing the CV curve of CuFeV LDH@GF with that of raw GF, it showed a larger peak area and higher current, demonstrating that the CuFeV LDH increases the rate of electron transfer on GF. This observation is consistent with previous reports of carbon-felt electrodes coated with catalysts [28]. The raw GF electrode exhibited no redox peak pairs, whereas the CuFeV LDH@GF electrode clearly showed oxidation–reduction pairs [29]. The enhanced rate of electron transfer on the CuFeV LDH@GF electrode significantly impacts its electrochemical efficiency and catalytic performance. The faster electron transfer kinetics facilitate more efficient exchange of electrons between the electrode and reactants in the electrochemical system, leading to more effective generation of $^{\bullet}OH$. Moreover, the improved electron transfer rate reduces overpotential losses, making the CuFeV LDH@GF electrode more energy-efficient and reducing electricity consumption during wastewater treatment.

The cathode activity toward the two-electron O_2 reduction reaction (ORR) affects the operation of the EF process. Therefore, a modified cathode should generate sufficient amounts of H_2O_2 for $^{\bullet}OH$ production. The electrocatalytic ORR activity of the developed cathode was evaluated using LSV (Figure 3f). The CuFeV LDH@GF cathode exhibited a higher current response in oxygen-saturated electrolytes compared to the pristine GF electrode. Additionally, the net current of the LSV curves of the modified electrode in N_2- and O_2-saturated environments confirmed the oxygen reduction activity and an enhanced ORR [30]. The onset of H_2 evolution reactions was observed to occur at a potential range of <-0.9 V/SCE in all cases. As the potential was raised from -0.2 to -0.8 V, the LSV curves obtained in the O_2-saturated system showed distinct reduction peaks and higher reductive current compared to those obtained in the system with N_2-saturated solutions [31]. The higher H_2O_2 production in the O_2-saturated

system than that in the N_2-saturated system was due to the maximal electrode activity for the two-electron reduction process of O_2 into H_2O_2 [32].

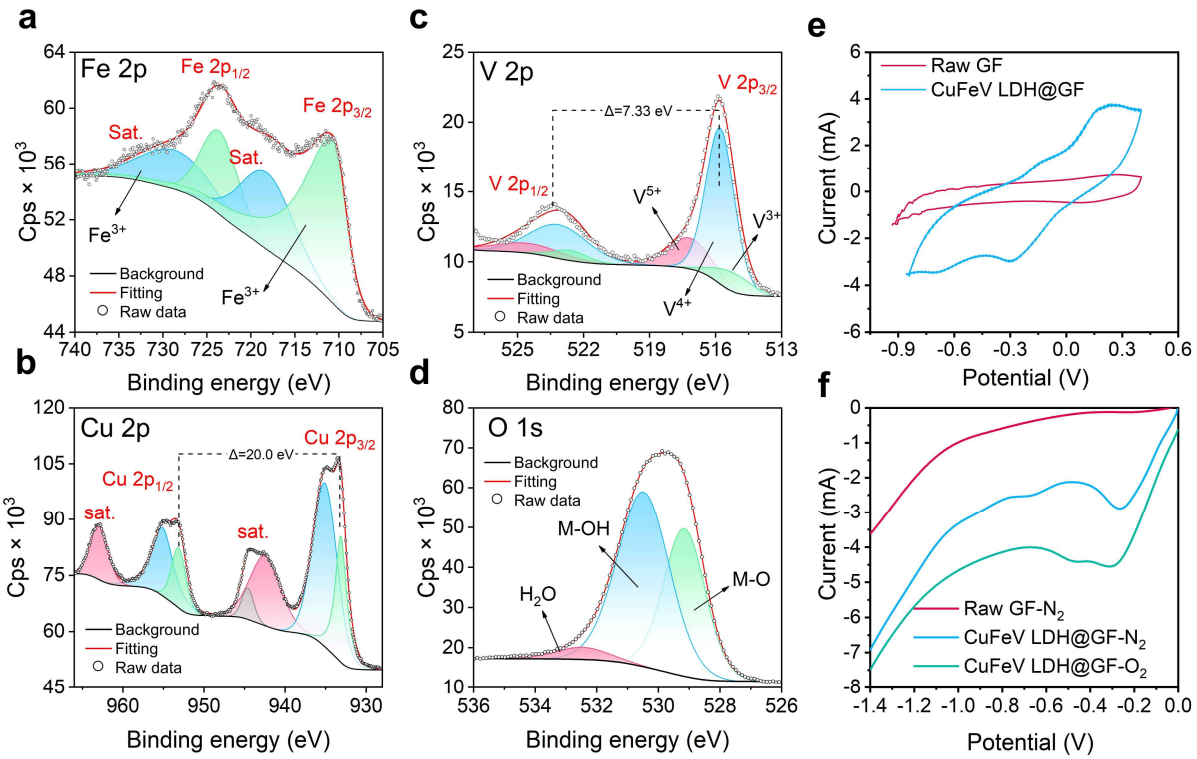

Figure 3. XPS profiles of the CuFeV LDH: a) Fe 2p, b) Cu 2p, c) V 2p, and d) O 1s; LSV and CV curves of raw GF and CuFeV LDH@GF.

As shown in Figure 4a, the pristine GF electrode produces 52.3 ± 2.5 mg L^{-1} H_2O_2 in 90 min, whereas the CuFeV@GF electrode produces 40.2 ± 3.5 mg L^{-1}. The higher H_2O_2 production of the GF electrode than that of the coated electrode could be due to the catalytic activation of H_2O_2 to produce ˙OH on the electrode surface [33]. Figure 4b and 4c show the UV–vis spectra of OPD-trapped •OH in the EF process with raw GF and CuFeV LDH@GF electrodes, respectively. Continuous production of ˙OH by the CuFeV LDH@GF electrode during the EF process was indicated by an increase in the intensity of the peak at 418 nm peak over time. The CuFeV LDH coating resulted in an increase in the generation of ˙OH during the EF process from 0.6 to 1.3 mM. (Figure 4d). Overall, considering ˙OH plays a vital role in the degradation

of organic pollutants, this enhanced •OH generation by CuFeV LDH@GF directly translates into greater LEV degradation efficiency.

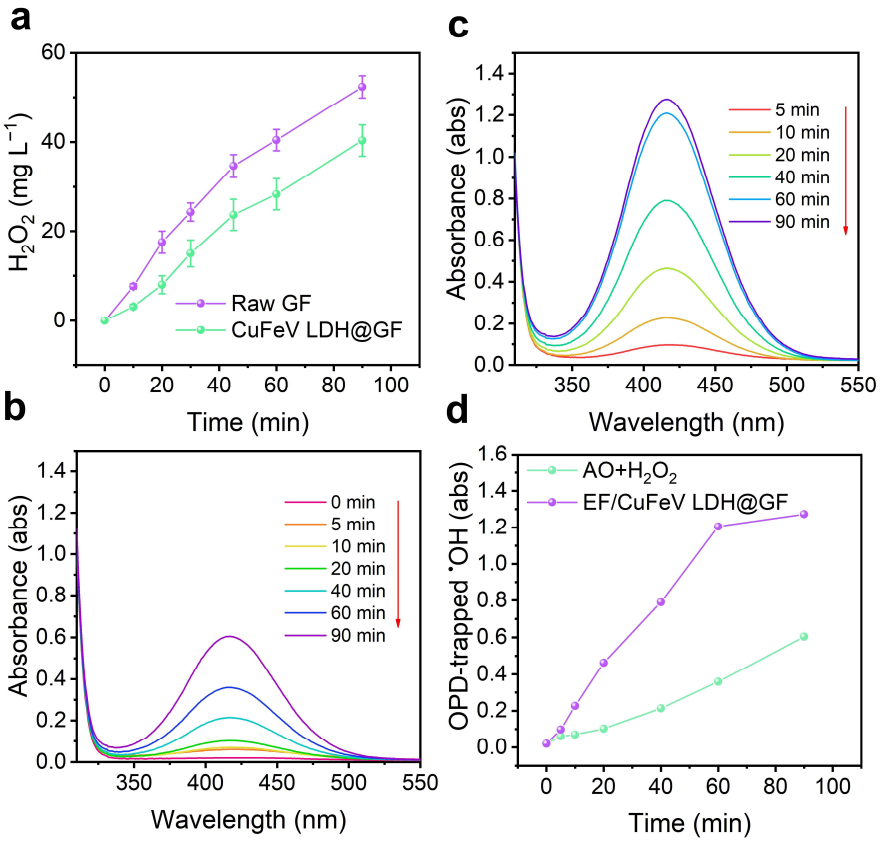

Figure 4. a) H_2O_2 production capabilities of raw and CuFeV LDH@GF cathodes; b) UV–vis spectra of OPD-trapped •OH in the EF process with raw GF and c) with CuFe@GF–EF process; absorbance of OPD–trapped •OH was measured at 418 nm (Experiment conditions: [LEV] = 15 mg L^{-1}, 1.5 V, pH = neutral, and [Na_2SO_4] = 50 mM).

3.2. Influence of the operating parameters

The efficiency of the EF process and the rate of H_2O_2 production were significantly dependent on the solution. Although the homogeneous Fenton reaction is known to be highly effective under acidic pH conditions, it is crucial to maintain a high process efficiency at near-neutral pH levels in the heterogeneous Fenton reaction [34]. The CuFeV@GF–EF process exhibits a good performance across a broad pH range, as illustrated in Figure 5a. It effectively removed

LEV with an efficiency of approximately 81.6% even under near-neutral pH conditions. However, when the pH was adjusted to 11, the performance of the CuFeV LDH@GF–EF process reduced, achieving only 64.9% efficiency. This decrease in performance at alkaline pH levels can be attributed to the low oxidation potential of •OH and the increase in the conversion rate of H_2O_2 into O_2 and H_2O [34]. The ability of the EF process to operate effectively across a wide pH range indicates that the process can withstand abrupt pH fluctuations, which are commonly encountered during real-time operation. When the initial concentration of LEV was increased from 15 to 30 mg L^{-1}, the performance of the CuFeV LDH@GF–EF process reduced (Figure 5b). At an initial LEV concentration of 15 mg L^{-1}, the process achieved a degradation efficiency of 80.3%. However, when the LEV concentration was increased to 30 mg L^{-1}, the removal efficiency decreased to 65%. This decrease in performance can be attributed to the constant production rate of •OH, which is insufficient to balance the increasing amount of LEV molecules. Furthermore, the excess LEV molecules may have obstructed the active sites of CuFeV LDH@GF, thereby inhibiting the catalytic decomposition of H_2O_2 to •OH [35]. In the EF process, the applied voltage governs the rate of H_2O_2 generation as well as drives the anodic oxidation of contaminants. The CuFeV LDH@GF–EF process efficiently degraded LEV at higher voltages, whereas a lower voltage resulted in a decreased performance (Figure 5c). The efficiency of the EF process for LEV degradation decreased below 40% at 1 V. A higher voltage also allows for the faster regeneration of the LDH catalyst, resulting in better process performance. Operating the process at a voltage of 2 V, LEV degradation was achieved with 90% efficiency. However, elevated voltages may lead to undesired side reactions, including competition between O_2 evolution and M(•OH) production on the anode, and suppression of the ORR at the cathode due to the hydrogen evolution reaction [36].

The contribution toward adsorption by the CuFeV LDH@GF electrode and anodic oxidation (AO) caused by the Pt anode was also investigated (Figures 5d and 5e). Adsorption by CuFeV

LDH@GF contributed to 20.6 ± 1.6 % LEV removal with a first-order reaction rate (k_{app}) constant of $3.9 \pm 0.5\times10^{-3}$ min^{-1}. In contrast, the AO+H_2O_2 process achieved an LEV removal efficiency of 59.3± 2.1 %, which might have been caused by the anodic oxidation of LEV and H_2O_2 oxidation. Notably, when the CuFeV LDH@GF electrode was used in the EF process, k_{app} increased from $15.3 \pm 0.9 \times 10^{-3}$ to $35.2 \pm 2.9\times10^{-3}$ min^{-1}. The process with CuFeV LDH@GF also exhibited a significantly higher rate constant in comparison to sum of the values achieved via individual processes ($19.2 \pm 0.4\times 10^{-3}$ min^{-1}). This substantial increase in the rate constant indicates a pronounced synergistic effect. The process had an SF of 1.83, demonstrating the potential of CuFeV LDH@GF as an efficient catalyst for the EF process. The EC of the CuFeV LDH@GF–EF process for the removal of LEV solution was 0.169 kWh m^{-3} and 9.75 ± 0.15 kWh $\cdot kg^{-1}$ LEV. In comparison, the EF process with raw GF achieved 35.6% greater EC with 13.22 ± 0.47 kWh $\cdot kg^{-1}$ LEV. The process also demonstrates a notable EC compared to those reported in existing literature, indicating a high energy efficiency.

3.3. Stability and reusability of CuFeV LDH@GF

Although the incorporation of a catalyst onto the cathode eliminates the requirement for a separate recovery step, the produced electrode should maintain its performance over repeated applications. To evaluate the reusability potential of the CuFeV LDH@GF electrode, we assessed the reduction in the LEV degradation percentage after 10 consecutive reuse runs (Figure 5f). The CuFeV LDH@GF electrode exhibited a decrease of 10.3% in LEV degradation after the 10^{th} application cycle. This decrease can be attributed to the gradual wearing off of the catalyst from the surface of GF during stirring or gas bubbling in the reactor.

Visual changes that occurred on the surface of the CuFeV LDH@GF electrode throughout the 10 reuse steps are presented in Figure S1.

In any water treatment process, preventing secondary pollution is of utmost importance. Concerns regarding heavy metal pollution are significant, particularly for catalysts with low stability. The concentrations of metals leached from the CuFeV LDH@GF cathode evaluated via ICP–OES were 0.018 mg L^{-1} of Cu, 0.001 mg L^{-1} of Fe, and 0.010 mg L^{-1} of V, all of which were substantially below the permissible limit prescribed by the World Health Organization [37].

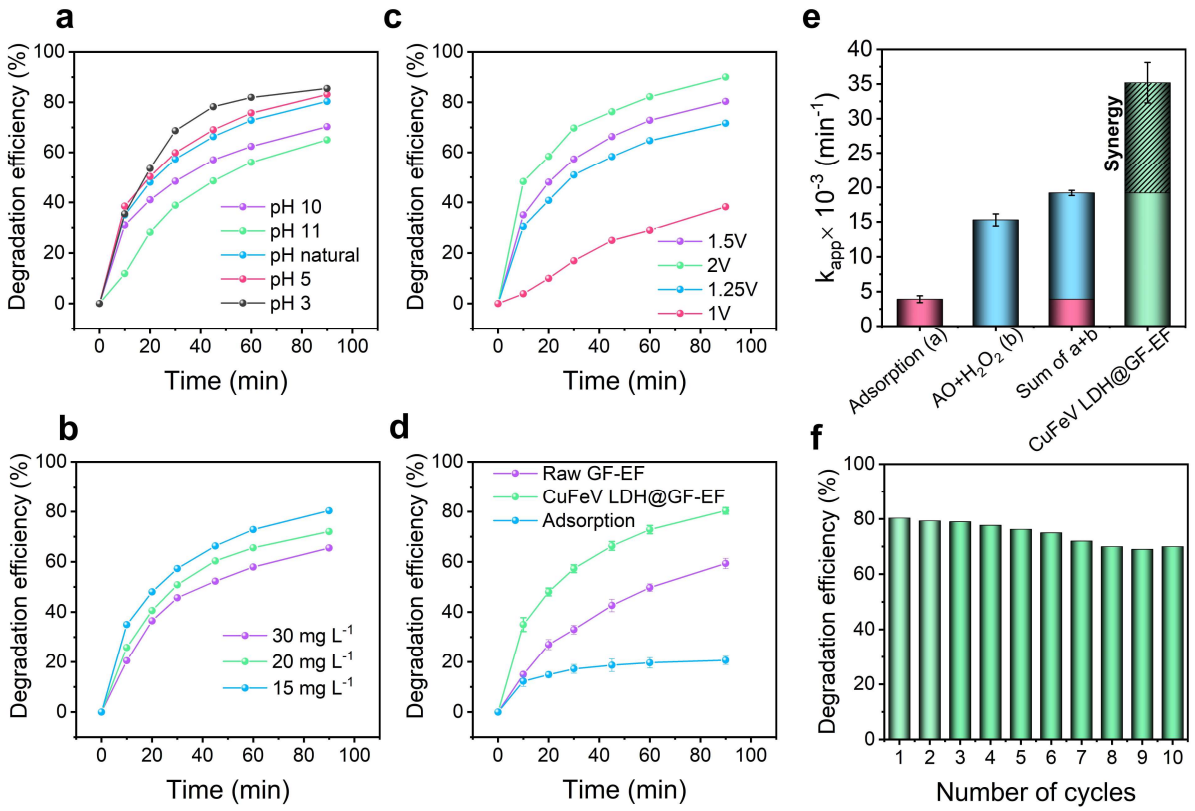

Figure 5. Influence of operating conditions on the performance of the EF process employing CuFeV LDH@GF in degrading LEV. a) solution pH, b) Initial LEV concentration, c) voltage, d) degradation of LEV in different process combinations, e) pseudo-first-order kinetic rate constants; and f) reusability of CuFeV LDH@GF over 10 reuse cycles (Experiment conditions: [LEV] = 15 mg L^{-1}, 1.5 V, pH = neutral, and [Na_2SO_4] = 50 mM).

3.4. Mechanism discussion

As cathode material, CuFeV LDH@GF initiates in-situ H_2O_2 production by two–electron reducing of O_2. Subsequently, the metal oxide-catalyzed decomposition of H_2O_2 generates $^{\bullet}OH$, following the principles of the Harber–Weiss theory [38]. At circumneutral pH, the surface-catalyzed activation of H_2O_2 occurs in the matrix of GF, where the octahedral sites of the CuFeV LDH are highly exposed [39]. As shown in XPS analysis, a high oxidation state (V^{4+}) is the most abundant form found in the CuFeV LDH, and its catalytic activity is expected to originate from these species [40]. The proposed mechanism of $^{\bullet}OH$ generation is based on electron transfer from redox couples of $\equiv Cu^{2+}/\equiv Cu^{3+}$, $\equiv Fe^{2+}/\equiv Fe^{3+}$and $\equiv V^{4+}/\equiv V^{5+}$ to H_2O_2 (Eqs. 4–6) [41,42]. Moreover, oxidized species ($\equiv Cu^{3+}$, $\equiv Fe^{3+}$, and $\equiv V^{5+}$)) can react with H_2O_2 to regenerate $\equiv Cu^{2+}$, $\equiv Fe^{2+}$, and $\equiv V^{4+}$ (Eqs. 7–9) [43]. Another contributor to the pollutant degradation is anodic oxidation on the Pt electrode (Eq. 10). GC–MS analysis of the intermediate products of LEV created during the CuFeV LDH@GF–EF process revealed eight intermediate products resulting from the opening of the aromatic ring, generating numerous different compounds (Table S1).

$$\equiv V^{4+} + H_2O_2 \rightarrow \equiv V^{5+} + OH^- + {}^{\bullet}OH \quad (4)$$

$$\equiv Fe^{2+} + H_2O_2 \rightarrow Fe^{3+} + OH^- + {}^{\bullet}OH \quad (5)$$

$$\equiv Cu^{2+} + H_2O_2 \rightarrow Cu^{3+} + OH^- + {}^{\bullet}OH \quad (6)$$

$$\equiv V^{5+} + H_2O_2 \rightarrow \equiv V^{4+} + HO_2^{\bullet} + H^+ \quad (7)$$

$$\equiv Fe^{3+} + H_2O_2 \rightarrow \equiv Fe^{2+} + HO_2^{\bullet} + H^+ \quad (8)$$

$$\equiv Cu^{3+} + H_2O_2 \rightarrow \equiv Cu^{2+} + HO_2^{\bullet} + H^+ \quad (9)$$

$$Pt + H_2O \rightarrow Pt({}^{\bullet}OH) + H^+ + e^- \quad (10)$$

$$LEV + {}^{\bullet}OH \rightarrow intermediates + H_2O \quad (11)$$

Similar synergistic affect has been reported in a previous study, in which the Cu-V bimetallic catalyst demonstrated higher catalytic activity, broader pH applicability, and improved

reusability compared to monometallic copper compounds in the degradation of fluconazole in heterogenous Fenton process [43]. The introduction of V into the copper-based catalyst enhanced various surface properties, such as adsorption capacity, surface defects, and active site concentration, leading to improved reactivity. In another study, the co-existence of Co^{2+}/Co^{3+}, Fe^{2+}/Fe^{3+}, and Ce^{3+}/Ce^{4+} couples in CoFeCe LDH grown carbon felt significantly improved the interfacial electron transfer to boost the generation of radical species through the decomposition of H_2O_2 [15]. Wang et al. (2018), showed that synergistic effect between Ni and Cu promoted the electron transfer from Ni^{2+} to Cu^{2+} through metal-oxo-meal bridged in the CuNiFe LDH. Additionally, the electron transfer from Cu^{2+} to Ni^{2+} made it possible to regeneration of Cu^{+}, further improving the efficiency of the Fenton reaction [12].

The potential toxicity of LEV and its degradation products was assessed using the ECOSAR software. Acute toxicity (LC_{50} or EC_{50}) and chronic toxicity of LEV and its degradation products is shown in Table S2. According to the classification criteria of the European Union for dangerous chemical substances (Directive 67/548/EEC), most degradation products and LEV were deemed harmless [44,45]. However, certain degradation products, such as D1 and D3, have potential acute and chronic toxicities. These findings highlight the importance of incorporating detoxification strategies in the effective treatment of emerging water contaminants, going beyond their mere removal.

4. Conclusions

In this study, we presented the successful synthesis and utilization of the CuFeV@GF electrode as a highly efficient and stable catalyst for the electro-Fenton process. The incorporation of two-dimensional flake-like LDH nanomaterials onto the electrode surface provided abundant active sites for the activation of in-situ generated H_2O_2. The importance of mixed valent states

for each metal (Fe, Cu, and V) contributed to the electrode's enhanced catalytic activity. Enhanced electron transfer kinetics and improved generation of •OH (1.27 mM) on the CuFeV LDH@GF electrode, resulted in an enhanced pollutant degradation efficiency. Notably, when the CuFeV LDH@GF electrode was used in the EF process, k_{app} increased from 15.3 ± 0.9 × 10^{-3} to 35.2 ± 2.9×10–3 min^{-1}. The electrode maintained its performance across a broad pH range, ensuring its applicability in diverse wastewater treatment scenarios. Furthermore, the CuFeV LDH@GF electrode demonstrated good reusability and efficiency throughout 10 consecutive reuse cycles. The CuFeV LDH@GF–EF process demonstrated an energy consumption (EC) of 0.169 kWh m^{-3} and 9.75 kWh $\cdot kg^{-1}$ LEV, which highlighting its favorable energy efficiency for the removal of LEV. These results emphasize the promising potential of this novel cathode as an alternative cathode for the remediation of water contaminated with emerging contaminants. The simple fabrication procedure further adds to its practical applicability.

Acknowledgment

We would like to thank the Scientific and Technical Research Council of Turkey (TUBITAK 2214–A, Application Number: 1059B142200017) for funding the research project. The authors are also grateful to Gebze Technical University, Yonsei University Mirae Campus and University of Tabriz for their support.

References

[1] T.A. Larsen, S. Hoffmann, C. Lüthi, B. Truffer, M. Maurer, Emerging solutions to the water challenges of an urbanizing world, Science (80-.). 352 (2016) 928–933.

[2] J. Liang, Y. Hou, H. Zhu, J. Xiong, W. Huang, Z. Yu, S. Wang, Levofloxacin degradation performance and mechanism in the novel electro-Fenton system constructed with vanadium oxide electrodes under neutral pH, Chem. Eng. J. 433 (2022) 133574. https://doi.org/10.1016/j.cej.2021.133574.

[3] D.B. Miklos, C. Remy, M. Jekel, K.G. Linden, J.E. Drewes, U. Hübner, Evaluation of advanced oxidation processes for water and wastewater treatment–A critical review, Water Res. 139 (2018) 118–131.

[4] S.O. Ganiyu, M. Zhou, C.A. Martínez-Huitle, Heterogeneous electro-Fenton and photoelectro-Fenton processes: A critical review of fundamental principles and application for water/wastewater treatment, Appl. Catal. B Environ. 235 (2018) 103–129. https://doi.org/10.1016/j.apcatb.2018.04.044.

[5] J. Wang, S. Li, Q. Qin, C. Peng, Sustainable and feasible reagent-free electro-Fenton via sequential dual-cathode electrocatalysis, Proc. Natl. Acad. Sci. U. S. A. 118 (2021) 1–7. https://doi.org/10.1073/pnas.2108573118.

[6] M. Liu, Z. Feng, X. Luan, W. Chu, H. Zhao, G. Zhao, Accelerated Fe2+ regeneration in an effective electro-fenton process by boosting internal electron transfer to a nitrogen-conjugated Fe (III) complex, Environ. Sci. Technol. 55 (2021) 6042–6051.

[7] S. Mehrabi-Kalajahi, A.O. Moghaddam, F. Hadavimoghaddam, M.A. Varfolomeev, A.L. Zinnatullin, I. Vakhitov, K.R. Minnebaev, D.A. Emelianov, D. Uchaev, A. Cabot, Entropy-stabilized metal oxide nanoparticles supported on reduced graphene oxide as a highly active heterogeneous catalyst for selective and solvent-free oxidation of toluene: a combined experimental and numerical investigation, J. Mater. Chem. A. 10 (2022) 14488–14500.

[8] S. Mehrabi-Kalajahi, Y. Orooji, S. Arefi-Oskoui, M.A. Varfolomeev, N.M. Khasanova, Y. Yoon, A. Khataee, Preparasion of layered V4AlC3 MAX phase for highly selective and efficient solvent-free aerobic oxidation of toluene to benzaldehyde, Mol. Catal. 529 (2022) 112545.

[9] L. Lv, Z. Yang, K. Chen, C. Wang, Y. Xiong, 2D Layered Double Hydroxides for Oxygen Evolution Reaction: From Fundamental Design to Application, Adv. Energy Mater. 9 (2019) 1–29. https://doi.org/10.1002/aenm.201803358.

[10] F. Dionigi, Z. Zeng, I. Sinev, T. Merzdorf, S. Deshpande, M.B. Lopez, S. Kunze, I. Zegkinoglou, H. Sarodnik, D. Fan, In-situ structure and catalytic mechanism of NiFe and CoFe layered double hydroxides during oxygen evolution, Nat. Commun. 11 (2020) 2522.

[11] B. Yao, Z. Luo, J. Yang, D. Zhi, Y. Zhou, FeIIFeIII layered double hydroxide modified carbon felt cathode for removal of ciprofloxacin in electro-Fenton process, Environ. Res. 197 (2021) 111144. https://doi.org/10.1016/j.envres.2021.111144.

[12] H. Wang, M. Jing, Y. Wu, W. Chen, Y. Ran, Effective degradation of phenol via Fenton reaction over CuNiFe layered double hydroxides, J. Hazard. Mater. 353 (2018) 53–61. https://doi.org/10.1016/j.jhazmat.2018.03.053.

[13] W. Yang, M. Zhou, N. Oturan, M. Bechelany, M. Cretin, M.A. Oturan, Highly efficient and stable FeIIFeIII LDH carbon felt cathode for removal of pharmaceutical ofloxacin

421 at neutral pH, J. Hazard. Mater. 393 (2020) 122513.
422 https://doi.org/10.1016/j.jhazmat.2020.122513.

423 [14] C. Xue, Z. Cao, X. Tong, P. Yang, S. Li, X. Chen, D. Liu, W. Huang, Investigation of
424 CuCoFe-LDH as an efficient and stable catalyst for the degradation of acetaminophen
425 in heterogeneous electro-Fenton system: Key operating parameters, mechanisms and
426 pathways, J. Environ. Manage. 327 (2023) 116787.
427 https://doi.org/10.1016/j.jenvman.2022.116787.

428 [15] M. Xu, J. Wei, X. Cui, J. Li, G. Pan, Y. Li, Z. Jiang, X. Niu, N. Cui, J. Li, High-efficiency
429 electro-Fenton process based on in-situ grown CoFeCe-LDH@CFs free-standing
430 cathodes: Correlation of cerium and oxygen vacancies with H2O2, Chem. Eng. J. 455
431 (2023) 140922. https://doi.org/10.1016/j.cej.2022.140922.

432 [16] G. Fang, W. Wu, C. Liu, D.D. Dionysiou, Y. Deng, D. Zhou, Activation of persulfate
433 with vanadium species for PCBs degradation: A mechanistic study, Appl. Catal. B
434 Environ. 202 (2017) 1–11. https://doi.org/10.1016/j.apcatb.2016.09.006.

435 [17] J. Liang, Y. Hou, J. Sun, H. Zhu, H. Pang, J. Yang, M. Wang, J. Sun, J. Xiong, W.
436 Huang, Z. Yu, S. Wang, Overpotential regulation of vanadium-doped chitosan carbon
437 aerogel cathode promotes heterogeneous electro-Fenton degradation efficiency, Appl.
438 Catal. B Environ. 317 (2022) 121794. https://doi.org/10.1016/j.apcatb.2022.121794.

439 [18] R. Keyikoğlu, A. Khataee, Y. Orooji, M. Kobya, Synergistic effect of Fe and Co metals
440 for the enhanced activation of hydrogen peroxide in the heterogeneous electro-Fenton
441 process by Co-doped ZnFe layered double hydroxide, J. Environ. Chem. Eng. (2022)
442 108875. https://doi.org/https://doi.org/10.1016/j.jece.2022.108875.

443 [19] K. Tada, M. Onoda, Nanostructured conjugated polymer films by electrophoretic
444 deposition, Adv. Funct. Mater. 12 (2002) 420–424.

445 [20] S. Wang, J. Zhu, S. Zhang, X. Zhang, F. Ge, Y. Xu, The catalytic degradation of
446 nitrobenzene by the Cu-Co-Fe-LDH through activated oxygen under ambient
447 conditions, Dalt. Trans. 49 (2020) 3999–4011. https://doi.org/10.1039/c9dt03794b.

448 [21] N. de M. Costa-Serge, R.G. Lima Gonçalves, M.A. Ramirez-Ubillus, C. Li, P. Hammer,
449 S. Chiron, R.F. Pupo Nogueira, Effect of the interlamellar anion on CuMgFe-LDH in
450 solar photo-Fenton and Fenton-like degradation of the anticancer drug 5-fluorouracil,
451 Appl. Catal. B Environ. 315 (2022) 121537.
452 https://doi.org/10.1016/j.apcatb.2022.121537.

453 [22] S. Nayak, G. Swain, K. Parida, Enhanced Photocatalytic Activities of RhB Degradation
454 and H2 Evolution from in Situ Formation of the Electrostatic Heterostructure
455 MoS2/NiFe LDH Nanocomposite through the Z-Scheme Mechanism via p-n
456 Heterojunctions, ACS Appl. Mater. Interfaces. 11 (2019) 20923–20942.
457 https://doi.org/10.1021/acsami.9b06511.

458 [23] Z. Wu, Y. ying Gu, S. Xin, L. Lu, Z. Huang, M. Li, Y. Cui, R. Fu, S. Wang, CuxNiyCo-
459 LDH nanosheets on graphene oxide: An efficient and stable Fenton-like catalyst for
460 dual-mechanism degradation of tetracycline, Chem. Eng. J. 434 (2022) 134574.
461 https://doi.org/10.1016/j.cej.2022.134574.

462 [24] Y. Vasseghian, D. Sezgin, D.C. Nguyen, H.Y. Hoang, M. Sari Yilmaz, A hybrid

nanocomposite based on CuFe layered double hydroxide coated graphene oxide for photocatalytic degradation of trimethoprim, Chemosphere. 322 (2023) 138243. https://doi.org/10.1016/j.chemosphere.2023.138243.

[25] P. Li, X. Duan, Y. Kuang, Y. Li, G. Zhang, W. Liu, X. Sun, Tuning Electronic Structure of NiFe Layered Double Hydroxides with Vanadium Doping toward High Efficient Electrocatalytic Water Oxidation, Adv. Energy Mater. 8 (2018) 1–8. https://doi.org/10.1002/aenm.201703341.

[26] K. Fan, H. Chen, Y. Ji, H. Huang, P.M. Claesson, Q. Daniel, B. Philippe, H. Rensmo, F. Li, Y. Luo, Nickel–vanadium monolayer double hydroxide for efficient electrochemical water oxidation, Nat. Commun. 7 (2016) 1–9.

[27] R. Keyikoglu, A. Khataee, H. Lin, Y. Orooji, Vanadium (V)-doped ZnFe layered double hydroxide for enhanced sonocatalytic degradation of pymetrozine, Chem. Eng. J. 434 (2022) 134730. https://doi.org/10.1016/j.cej.2022.134730.

[28] L. Xie, X. Mi, Y. Liu, Y. Li, Y. Sun, S. Zhan, W. Hu, High Efficient Degradation of Polyacrylamide by Fe-doped Ce0.75Zr0.25O2 Solid Solution / CF Composite Cathode in Heterogeneous Electro-Fenton Process, ACS Appl. Mater. Interfaces. 11 (2019) 30703–30712. https://doi.org/10.1021/acsami.9b06396.

[29] N.T. Dung, L.T. Duong, N.T. Hoa, V.D. Thao, L.V. Ngan, N.N. Huy, A comprehensive study on the heterogeneous electro-Fenton degradation of tartrazine in water using CoFe2O4/carbon felt cathode, Chemosphere. 287 (2022). https://doi.org/10.1016/j.chemosphere.2021.132141.

[30] Y. Zhu, S. Qiu, F. Deng, Y. Zheng, K. Li, F. Ma, D. Liang, Enhanced degradation of sulfathiazole by electro-Fenton process using a novel carbon nitride modified electrode, Carbon N. Y. 145 (2019) 321–332. https://doi.org/10.1016/j.carbon.2019.01.032.

[31] T.X.H. Le, M. Bechelany, S. Lacour, N. Oturan, M.A. Oturan, M. Cretin, High removal efficiency of dye pollutants by electron-Fenton process using a graphene based cathode, Carbon N. Y. 94 (2015) 1003–1011. https://doi.org/10.1016/j.carbon.2015.07.086.

[32] W. Lai, G. Xie, R. Dai, C. Kuang, Y. Xu, Z. Pan, L. Zheng, L. Yu, S. Ye, Z. Chen, H. Li, Kinetics and mechanisms of oxytetracycline degradation in an electro-Fenton system with a modified graphite felt cathode, J. Environ. Manage. 257 (2020) 109968. https://doi.org/10.1016/j.jenvman.2019.109968.

[33] H. Qi, X. Sun, Z. Sun, Cu-doped Fe2O3 nanoparticles/etched graphite felt as bifunctional cathode for efficient degradation of sulfamethoxazole in the heterogeneous electro-Fenton process, Chem. Eng. J. 427 (2021) 131695. https://doi.org/10.1016/j.cej.2021.131695.

[34] Q. Yan, C. Lian, K. Huang, L. Liang, H. Yu, P. Yin, J. Zhang, M. Xing, Constructing an acidic microenvironment by MoS2 in heterogeneous Fenton reaction for pollutant control, Angew. Chemie Int. Ed. 60 (2021) 17155–17163.

[35] X. Hou, X. Huang, F. Jia, Z. Ai, J. Zhao, L. Zhang, Hydroxylamine promoted goethite surface Fenton degradation of organic pollutants, Environ. Sci. Technol. 51 (2017) 5118–5126.

[36] L. Cui, M. Sun, Z. Zhang, Flow-through integration of FeOCl/graphite felt-based heterogeneous electro-Fenton and Ti4O7-based anodic oxidation for efficient contaminant degradation, Chem. Eng. J. 450 (2022) 138263. https://doi.org/10.1016/j.cej.2022.138263.

[37] W.H.O. WHO Press, Guidelines for Drinking-water Quality, fourth ed., Geneva, Switzerland, 2011.

[38] F. Haber, J. Weiss, The catalytic decomposition of hydrogen peroxide by iron salts, Proc. R. Soc. London. Ser. A-Mathematical Phys. Sci. 147 (1934) 332–351.

[39] S.O. Ganiyu, T.X. Huong Le, M. Bechelany, N. Oturan, S. Papirio, G. Esposito, E. van Hullebusch, M. Cretin, M.A. Oturan, Electrochemical mineralization of sulfamethoxazole over wide pH range using Fe II Fe III LDH modified carbon felt cathode: Degradation pathway, toxicity and reusability of the modified cathode, Chem. Eng. J. 350 (2018) 844–855. https://doi.org/10.1016/j.cej.2018.04.141.

[40] X. Liang, S. Zhu, Y. Zhong, J. Zhu, P. Yuan, H. He, J. Zhang, The remarkable effect of vanadium doping on the adsorption and catalytic activity of magnetite in the decolorization of methylene blue, Appl. Catal. B Environ. 97 (2010) 151–159.

[41] J. Deng, J. Jiang, Y. Zhang, X. Lin, C. Du, Y. Xiong, FeVO4 as a highly active heterogeneous Fenton-like catalyst towards the degradation of Orange II, Appl. Catal. B Environ. 84 (2008) 468–473. https://doi.org/10.1016/j.apcatb.2008.04.029.

[42] G. Fang, Y. Deng, M. Huang, D.D. Dionysiou, C. Liu, D. Zhou, A Mechanistic Understanding of Hydrogen Peroxide Decomposition by Vanadium Minerals for Diethyl Phthalate Degradation, Environ. Sci. Technol. 52 (2018) 2178–2185. https://doi.org/10.1021/acs.est.7b05303.

[43] N. Zhang, C. Xue, K. Wang, Z. Fang, Efficient oxidative degradation of fluconazole by a heterogeneous Fenton process with Cu-V bimetallic catalysts, Chem. Eng. J. 380 (2020) 122516. https://doi.org/10.1016/j.cej.2019.122516.

[44] C. Directive, Council Directive 67/548/EEC of 27 June 1967 on the approximation of laws, regulations and administrative provisions relating to the classification, packaging and labelling of dangerous substances, Off. J. Eur. Communities. 196 (1967) 1.

[45] GHS (United Nations), Globally harmonized system of classification and labelling of chemicals (GHS)(4th Edition), 2021.